

# Structure and stability of discrete breather in zigzag and armchair carbon nanotubes

Y. Doi<sup>†</sup>, A. Nakatani

<sup>†</sup>doi@ams.eng.osaka-u.ac.jp

Department of Adaptive Machine Systems, Graduate School of Engineering, Osaka University, 2-1 Yamadaoka, Suita, Osaka, 565-0871, Japan

Structure and stability of stationary discrete breathers (DBs) in armchair and zigzag carbon nanotubes (CNTs) are investigated numerically. Precise numerical solutions of DB in CNTs are calculated by a numerical method that couples the Newton-Raphson method and molecular dynamics method. Linear stability analysis is performed by constructing of monodromy matrix of the numerical solution of DB from the numerical results of MD simulation. In both structures of zigzag and armchair carbon nanotube, stationary DBs with higher angular frequency above zone boundary mode exist. Displacement of DB is on cylindrical plane of CNTs. Linear stability analysis shows that DBs in both armchair CNT and zigzag CNT are unstable. The maximum growth rate of the unstable perturbation mode can be calculated numerically. The maximum growth rate of armchair CNT is greater than that of zigzag CNT even when the curvature of the cylindrical plane of zigzag CNT is greater than armchair CNT. In both case of armchair and zigzag CNT, the unstable motion is excited in the direction out of the cylindrical plane of CNTs. Unstable dynamics is suppressed by introducing extensive strain in axial direction of CNT. In this case, motion of the unstable perturbation modes is confined on the cylindrical plane of CNTs.

**Keywords:** discrete breather, intrinsic localized mode, carbon nanotube.

## 1. Introduction

In nonlinear lattices, it has been known that spatial localized modes called discrete breathers (DBs) or intrinsic localized modes (ILMs) can be excited out of the dispersion bands of the lattices. Since the first report of DB by Sievers and Takeno[1], a variety of theoretical and numerical investigations on DB has been performed[2, 3]. Recently, observations of DBs in physical systems such as micromechanical systems[4], macromechanical systems[5], magnet-mechanical systems[6], electrical lattices[7] and optical lattices[8] have been reported. These reports indicate that DB does exist in the real systems and that DB can play physical roles in these systems.

One of the most attractive subjects of DBs in the physical systems is those in materials. Because crystal has discrete structure and interaction between atoms is anharmonic, it has been expected that DBs exist in material as vibration modes in atomic scales. Excitation of DBs in material has been attracted since the early stage of study of DB[9-16]. Interaction between DBs and structures in crystal such as vacancy, dislocation and impurity has been also investigated[17-20].

Recently, DB in carbon nanostructure has been extensively investigated[21]. As to graphene, spontaneous excitation of DB[22], structure and stability of DB[23], excitation of DB at edge boundary of graphene[24] have been studied numerically. Recently energy exchange of DB in graphene has been also reported[25]. Moreover, excitation of DB in carbon nanotube(CNT) has been investigated numerically[26-28]. Discussion of a physical role of DB

in Stone-Wales transformation in CNT[29] indicates importance of understanding of dynamics DB in crystal.

In this paper, we investigate structure and stability of DB in CNTs. Understanding of stability of DB in CNT is the first step of understanding of DB dynamics and physical process due to DB.

## 2. Models and numerical method

Atomic models for CNT are considered for molecular dynamics (MD) simulations. The CNT is formed by wrapping a graphene in a specific direction ( $n, m$ ). The parameters  $n$  and  $m$  represents the number of unit vectors which requires for closing seamlessly a boundary of graphene. When  $m = 0$ , the CNT is called zigzag CNT. When  $n = m$ , on the other hand, the CNT is called armchair CNT. In this study, we consider two different configurations of CNT: armchair CNT (10, 10) and zigzag CNT (10, 0).

In atomic simulations, interatomic potential is required to describe dynamics of atoms. In this study, we consider widely used empirical potential for hydrocarbon system proposed by Brenner[30]. The Brenner potential takes the following form,

$$H = \sum_{n=1}^{3N} \frac{p_n^2}{2M} + \frac{1}{2} \sum_i^N \sum_{j \neq i}^N \sum_{k \neq i, j}^N \Phi_{ijk}(r_{ij}, r_{jk}, \theta_{ijk}), \quad (1)$$

where  $M$  is mass of carbon atom,  $p_n$  is the momentum in the phase space,  $\Phi_{ijk}$  is interaction potential,  $r_{ij}$  ( $r_{jk}$ ) is distance between  $i$ -th and  $j$ -th ( $j$ -th and  $k$ -th) atoms,  $\theta_{ijk}$  is angle between  $i$ - $j$  and  $i$ - $k$  bonds. The function  $\Phi_{ijk}$  is determined in order to describe macroscopic properties of carbon structure.

In the atomic system, periodic boundary condition is considered in  $x$ -,  $y$ -, and  $z$ -direction. In  $x$  and  $y$  coordinates, box size is so large that interaction between mirror atoms can be negligible. We consider energy conservation system. Therefore, no heat bath is connected to the system. Numerical integration of the equation of motion is performed by the velocity Verlet method. The time step of the numerical integration is 0.1fs.

The equations of motions is given by

$$\frac{dq_n}{dt} = \frac{\partial H}{\partial p_n}, \quad (2)$$

$$\frac{dp_n}{dt} = -\frac{\partial H}{\partial q_n}. \quad (3)$$

Let  $\mathbf{X}(t) = (q_1(t), q_2(t), \dots, q_{3N}(t), p_1(t), p_2(t), \dots, p_{3N}(t))$  be a state variable in the phase space. The equation of motion (2) and (3) can be linearized around  $\mathbf{X}(t)$ .

$$\frac{d\xi_n}{dt} = \sum_{m=1}^{3N} \frac{\partial^2 H}{\partial p_n \partial q_m} \Big|_{\mathbf{X}} \xi_m + \sum_{m=1}^{3N} \frac{\partial^2 H}{\partial p_n \partial p_m} \Big|_{\mathbf{X}} \zeta_m, \quad (4)$$

$$\frac{d\zeta_n}{dt} = -\sum_{m=1}^{3N} \frac{\partial^2 H}{\partial q_n \partial q_m} \Big|_{\mathbf{X}} \xi_m + \sum_{m=1}^{3N} \frac{\partial^2 H}{\partial q_n \partial p_m} \Big|_{\mathbf{X}} \zeta_m, \quad (5)$$

where  $\xi_m(t)$  and  $\zeta_m(t)$  are small variation around  $q_n(t)$  and  $p_n(t)$ , respectively.

The temporal evolution of  $\mathbf{X}(t+t')$  from the state  $\mathbf{X}(t)$  in the phase space is written as

$$\mathbf{X}(t+t') = \mathcal{A}_{t'}(\mathbf{X}). \quad (6)$$

Using Eq. (6), difference between the initial state  $\mathbf{X}(t)$  and its temporal evolution at  $t'$  can be written as

$$\mathbf{D}(\mathbf{X}) = \mathcal{A}_{t'}(\mathbf{X}) - \mathbf{X}. \quad (7)$$

Precise numerical solutions of DB in CNT is a periodic orbit described by (2) and (3) in the phase space. If  $\mathbf{X}_0$  is on the periodic orbit with a period  $T$ , we obtain

$$\mathbf{D}(\mathbf{X}_0) = \mathcal{A}_T(\mathbf{X}_0) - \mathbf{X}_0 = \mathbf{0}. \quad (8)$$

Let  $\mathbf{X}_n$  be a point near the orbit of periodic solution and  $\delta\mathbf{X}$  be a correction vector to the precise solution. The correction vector  $\delta\mathbf{X}$  can be obtained by substituting  $\mathbf{X}_n + \delta\mathbf{X}$  into (8) and Taylor expansion as follows:

$$\delta\mathbf{X} = -(\partial\mathcal{A}_T(\mathbf{X}_n) - I)^{-1}(\mathcal{A}_T(\mathbf{X}_n) - \mathbf{X}_n), \quad (9)$$

where  $I$  is the unit matrix and  $\partial\mathcal{A}_T(\mathbf{X})$  is a tangential map defined as follows:

$$\partial\mathcal{A}_T(\mathbf{X}) = \begin{pmatrix} \frac{\partial A_1}{\partial q_1} & \frac{\partial A_1}{\partial q_2} & \dots & \frac{\partial A_1}{\partial p_{3N}} \\ \frac{\partial A_2}{\partial q_1} & \frac{\partial A_2}{\partial q_2} & \dots & \frac{\partial A_2}{\partial p_{3N}} \\ \vdots & \vdots & \ddots & \vdots \\ \frac{\partial A_{6N}}{\partial q_1} & \frac{\partial A_{6N}}{\partial q_2} & \dots & \frac{\partial A_{6N}}{\partial p_{3N}} \end{pmatrix}. \quad (10)$$

Precise numerical solutions of DB in CNT can be calculated by Newton-Raphson method updating the correction vector  $\delta\mathbf{X}$  with (9). The orbit  $\mathbf{X}_n$  is obtained from the numerical integration of (2) and (3). The tangential map (10) can be calculated numerically by

$$\frac{\mathcal{A}_T(\mathbf{X} + \Delta\zeta_n) - \mathcal{A}_T(\mathbf{X} - \Delta\zeta_n)}{2\Delta}, \quad (11)$$

where  $\Delta$  is a small parameter,  $\zeta_n$  is a vector defined by

$$\zeta_1 = (1, 0, 0, \dots, 0)^T, \zeta_2 = (0, 1, 0, \dots, 0), \dots, \zeta_{6N} = (0, 0, 0, \dots, 1). \quad (12)$$

Once the precise numerical solution of DB in CNT is obtained, linear stability analysis of the DB is also investigated. The linearized equation around the solution of DB is given by (4) and (5). These equations are differential equations with  $T$ -periodic coefficients:

$$\frac{d\zeta}{dt} = C(t)\zeta, \quad (13)$$

$$C(t) = C(t+T). \quad (14)$$

Solution of (13) and (14) holds following relation:

$$\zeta(t+T) = M(T)\zeta(t), \quad (15)$$

where  $M(T)$  is  $6N \times 6N$  matrix called monodromy matrix. Let  $\sigma_m$  be eigenvalue of the monodromy matrix  $M(T)$  and let  $\psi_m$  be eigenvector of  $M(T)$ .

$$\sigma_m M(T) = \psi_m M(T). \quad (16)$$

The eigenvalue  $\sigma_m$  indicates growth rate of  $m$ -th perturbation mode around the DB and the eigenvector  $\psi_m$  indicates displacement pattern of  $m$ -th perturbation mode. In Hamilton systems, if  $\sigma_m$  is an eigenvalue,  $1/\sigma_m$  is also an eigenvalue. Therefore, the precise solution of DB is stable if and only if all eigenvalues is on the unit circle in the imaginary plane.

The numerical representation of the monodromy matrix is obtained from the numerical integration of the linearized equations. Each row of the monodromy matrix can be calculated numerically by integrating the linearized equations (4) and (5) from  $t=0$  to  $t=T$  with  $6N$ -initial conditions (12).

### 3. Numerical results and discussion

Precise numerical solutions of DB in CNT are obtained by Newton-Raphson method. Structures of DB in armchair CNT and zigzag CNT are shown in Fig. 1 and Fig. 2, respectively. In each case, period of DB is 18ps. In the case of armchair CNT, DB in the bond along to circumference direction is possible. In the case of zigzag CNT, on the other hand, DB in the bond along to axial direction is possible. It is observed that two atoms in DB vibrate with large amplitude. However, surrounding four atoms also slightly vibrate. Structure of precise solution of DB is similar to those observed in MD simulation [26].

Linear stability analysis is also performed. As far as our results, all DB is linearly unstable in zigzag CNT and armchair CNT. Figure 3 shows the relation between the maximum growth rate of unstable mode around DB and its period. DB becomes more unstable when the period of DB becomes longer. Growth rate of DB in zigzag CNT is larger than that in armchair CNT. In our calculations, diameter of zigzag CNT is smaller than that of armchair CNT. This means that a curvature of armchair CNT is smaller than that of zigzag CNT. Even in the case of smaller curvature than zigzag CNT, the most unstable mode of DB in the armchair CNT has larger growth rate than that in the zigzag CNT. This results are consistent with the results of our previous study on

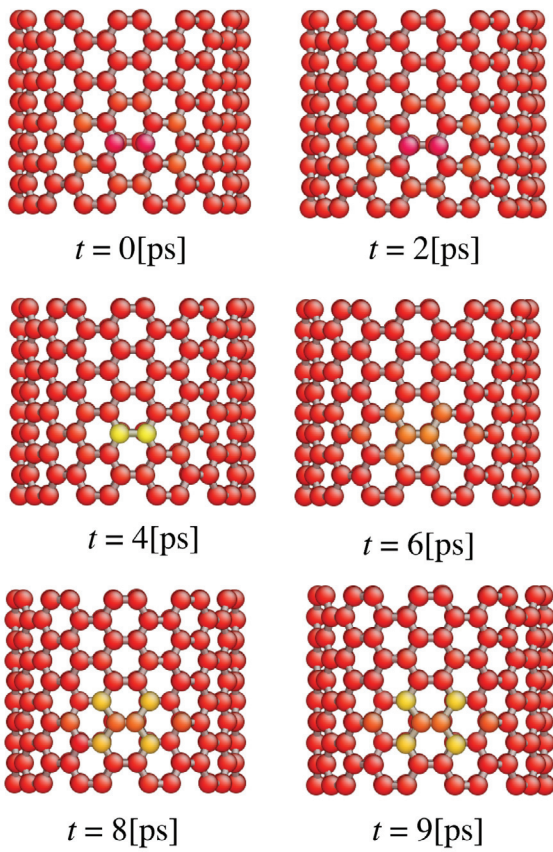


Fig. 1. (Color online) Structure of DB in armchair CNT.

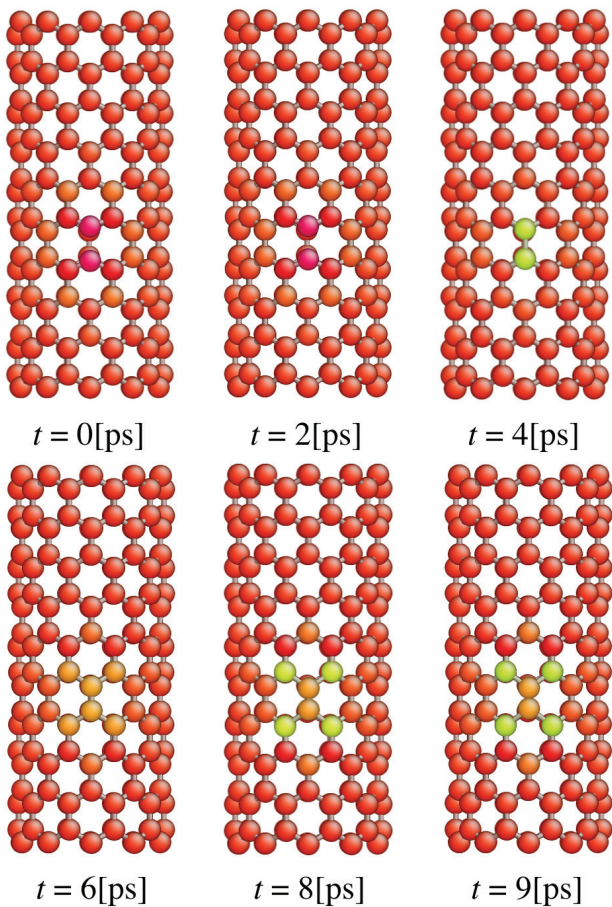


Fig. 2. (Color online) Structure of DB in zigzag CNT.

MD simulation of DB in CNTs which shows the DB in zigzag CNT has shorter lifetime than the DB in armchair CNT [26].

Displacement pattern of the unstable perturbation modes with maximum growth rate in armchair CNT and zigzag CNT is presented in Fig. 4 and Fig. 5, respectively. Unstable motion is excited around DB. In both cases, motion of unstable perturbation modes is out of the cylindrical plane of CNTs. This is contrast to that the vibration of DB is on the cylindrical plane of CNTs.

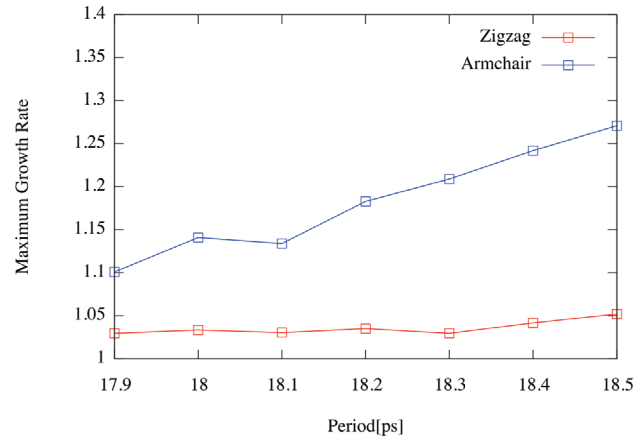


Fig. 3. Maximum growth rate of DB in CNT.

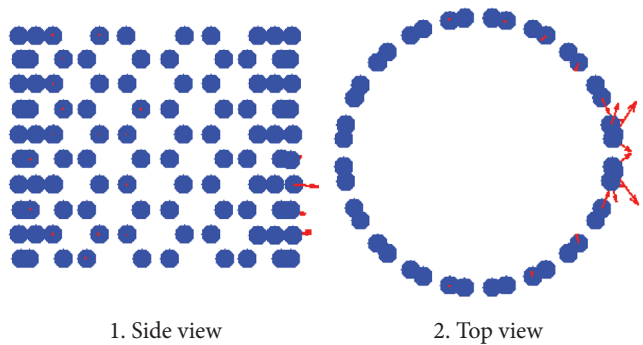


Fig. 4. Displacement pattern of unstable perturbation mode with the maximum growth rate in armchair CNT.

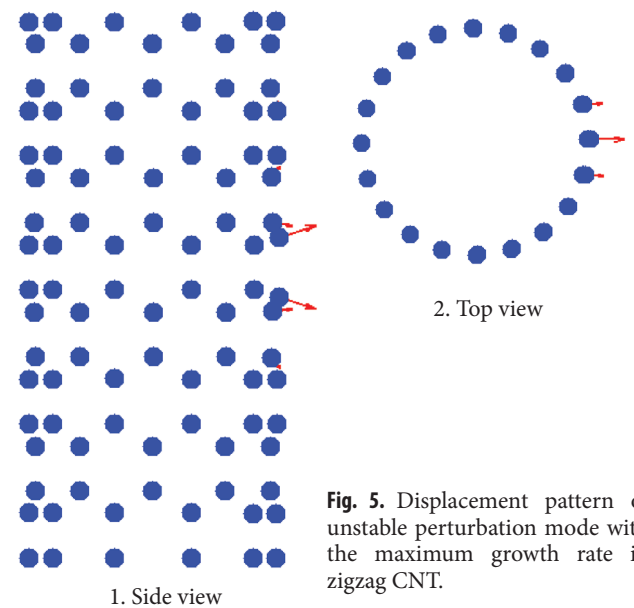


Fig. 5. Displacement pattern of unstable perturbation mode with the maximum growth rate in zigzag CNT.

When the axial strain is applied to the CNTs, growth rate changes drastically. Table 1 shows change of the maximum growth rate of perturbation mode of DB with period  $T = 18\text{ps}$  after applying strain to zigzag CNT and armchair CNT, respectively. When compressive strain is applied, the maximum growth rate becomes larger than the case without strain in the zigzag CNT and smaller than the same without strain in the armchair CNT. When extensive strain is applied to CNTs, on the other hand, the maximum growth rate becomes smaller in the both cases of zigzag CNT and armchair CNT. This tendency is also observed in DBs with other period  $T$ . Therefore, as far as our knowledge, extensive axial strain to the CNT suppresses the instability of DB in CNTs. In other word, DBs in CNT have longer lifetime by applying extensive strain to the zigzag CNT and armchair CNT. Longer lifetime of DB in crystals is important for possible physical process due to DB, since longer lifetime of DB makes possibility of physical process due to DB larger.

Another drastic effect due to strain to CNTs is change of the displacement pattern of unstable perturbation modes shown in Fig. 6 and Fig. 7. It is found that vibration of the unstable perturbation modes with the maximum growth rate are confined on the cylindrical plane. This is contract to that vibration are oriented to out of the cylindrical plane.

#### 4. Conclusion

In this study, we investigate the structure and dynamics of DB in armchair CNT and zigzag CNT. By using numerical method which couples MD method and Newton-Raphson method, the precise numerical solutions of DB can be obtained for both armchair CNT and zigzag CNT. It is found that DB in CNTs is linearly unstable and the unstable modes with maximum growth rate vibrate in direction out of cylindrical plane of CNTs. It is confirmed that the maximum growth rate of unstable perturbation mode of armchair CNT is larger than that of zigzag CNT. This is consistent with our previous report. Finally, it is found that the instability of DB is suppressed by introducing extensive axial strain to CNTs. In this case, the unstable motion out of the cylindrical plane of CNT is also suppressed.

By using our method for finding the precise numerical solutions of DB in CNT, it can be expected to find other DB solution of different symmetry. Moreover, it is expected to find DB solution in other configuration of CNT such as chiral CNTs. These problems are left for future investigations.

#### References

1. A. J. Sievers, S. Takeno. Phys. Rev. Lett. **61**, 970 (1988).
2. S. Flach, A. V. Gorbach. Phys. Rep. **467**, 1 (2008).
3. K. Yoshimura, Y. Doi, M. Kimura. Localized modes in nonlinear discrete systems. in "Progress in Nanophotonics 3" (M. Ohtsu, T. Yatsui (eds.)), pp. 119–166 (2015).
4. M. Sato, B.E. Hubbard, A.J. Sievers, B. Ilic, D.A. Czaplewski, H.G. Craghead. Phys. Rev. Lett. **90**, 044102 (2003).

5. Y. Watanabe, T. Nishida, N. Sugimoto. Proceedings of the Estonian Academy of Sciences. **64**, pp.417–212 (2015).
6. M. Kimura, T. Hikihara. Chaos. **19**, 013138 (2009).
7. L.Q. English, F. Palmero, A.J. Sievers, P.G. Kevrekidis, D.H. Barnak. Phys. Rev. E. **81** (4), 046605 (2010).
8. H. S. Eisenberg, Y. Silberberg, R. Morandotti, A. R. Boyd, J.S. Aitchison. Phys. Rev. Lett. **81**, 3383 (1998).
9. S. A. Kiselev, S. R. Bickham, A. J. Sievers. Phys. Rev. B. **50**, 9135 (1994).
10. S.A. Kiselev, A.J. Sievers. Phys. Rev. Lett. **55** (9) 5755 (1997).
11. S. V. Dmitriev. Letters on Materials. **1** (2), 78 (2011).
12. A. A. Kistanov, S. V. Dmitriev. Physics of the Solid State. **54** (8), 1648 (2012).
13. A. A. Kistanov, R. T. Murzaev, S. V. Dmitriev, V. I. Dubinko, V. V. Khizhnyakov. JETP Letters. **99** (6), 353 (2014).

**Table 1.** Change of maximum growth rate after applying strain to CNT.

Strain	zigzag CNT	armchair CNT
e=0%	1.034	1.141
e=+1%	1.020	1.016
e=-1%	1.039	1.028

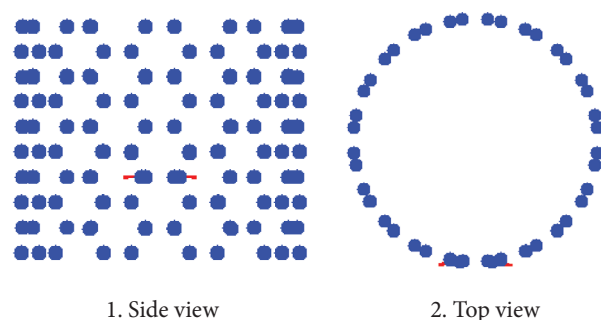


**Fig. 6** Displacement pattern of unstable perturbation mode in armchair CNT with extensive axial strain

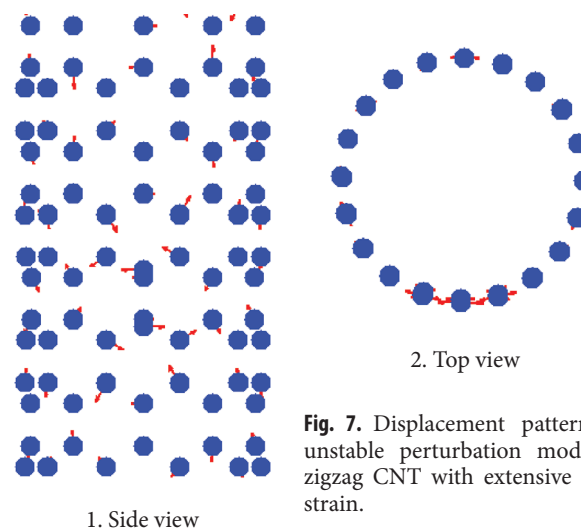


**Fig. 7.** Displacement pattern of unstable perturbation mode in zigzag CNT with extensive axial strain.

14. S.V. Dmitriev, A.A. Kistanov, V.I. Dubinko. Moving Discrete Breathers in 2D and 3D Crystals in “Quodons in Mica” (J.F.R. Archilla, N. Jeménez, V.J. Sánchez-Morcillo, L.M. García-Raffi. eds.), pp.205–227 (2015).
15. R.T. Murzaev, A.A. Kistanov, V.I. Dubinko, D.A. Terentyev, S.V. Dmitriev. *Computational Material Science*. **98**, 88 (2015).
16. M.D. Starostenkov, A.I. Potekaev, S.V. Dmitriev, P.V. Zakharov, A.M. Erimin, V.V. Kulagina. *Russian Physics Journal*. **58** (9), 1353 (2016).
17. J.L. Marín, J.C. Eilbeck, F.M. Russel, *Phys. Lett. A*. **248**, 225 (1998).
18. J. Cuevas, C. Katerji, J.F. R. Archilla, J.C. Eilbeck, F.M. Russel. *Phys. Lett. A*. **315**, 364 (2003).
19. J. Bajars, J.C. Eilbeck, B. Leimkuhler. *Physica D*. **301–302**, 8 (2015).
20. J. Bajars, J.C. Eilbeck, B. Leimkuhler. Numerical Simulations of Nonlinear Modes in Mica: Past, Present and Future in “Quodons in Mica” (J.F.R. Archilla, N. Jeménez, V.J. Sánchez-Morcillo, L.M. García-Raffi. eds.), pp 35–67 (2015).
21. J.A. Baimova, E.A. Korznikova, I.P. Lobzenko, S.V. Dmitriev. *Reviews on Advanced Materials Science*. **42** (1), 68 (2015).
22. Y. Yamayose, Y. Kinoshita, Y. Doi, A. Nakatani, T. Kitamura. *EPL*. **80**, 40008 (2007).
23. Y. Doi, A. Nakatani. *Journal of Solid Mechanics and Materials Engineering*. **6** (1), 71 (2012).
24. E.A. Korznikova, A.V. Savin, Yu. A. Baimova, S.V. Dmitriev, R.R. Mulyukov. *JETP Letters*. **96** (4), 222 (2012).
25. J.A. Baimova, S.V. Dmitriev. *Russian Physics Journal*. **58** (6), 785 (2015).
26. Y. Kinoshita, Y. Yamayose, Y. Doi, A. Nakatani, T. Kitamura. *Phys. Rev. B*. **77**, 024307 (2008).
27. T. Shimada, D. Shirasaki, Y. Kinoshita, Y. Doi, A. Nakatani, T. Kitamura. *Physica D*. **239**, 407 (2010).
28. Y. Doi, A. Nakatani. *Proc. of 2015 International Symposium of Nonlinear Theory and its Applications (NOLTA2015)*. Hong Kong. No. 6259 (2015).
29. T. Shimada, D. Shirasaki, T. Kitamura. *Phys. Rev. B*. **81**, 035401 (2010).
30. D.W. Brenner. *Phys. Rev. B*. **42** (15), 9458 (1990).